J. Fluid Mech. (2010), *vol.* 661, *pp.* 294–315.
doi:10.1017/S0022112010003046

Transition to global instability in transverse-jet shear layers

J. DAVITIAN, D. GETSINGER, C. HENDRICKSON AND A. R. KARAGOZIAN†

Department of Mechanical and Aerospace Engineering, University of California, Los Angeles, CA 90095-1597, USA

(Received 12 June 2009; revised 24 May 2010; accepted 25 May 2010; first published online 27 July 2010)

In a recent paper (Megerian *et al.*, *J. Fluid Mech.*, vol. 593, 2007, pp. 93–129), experimental exploration of the behaviour of transverse-jet near-field shear-layer instabilities suggests a significant change in the character of the instability as jet-to-crossflow velocity ratios R are reduced below a critical range. The present study provides a detailed exploration of and additional insights into this transition, with quantification of the growth of disturbances at various locations along and about the jet shear layer, frequency tracking and response of the transverse jet to very strong single-mode forcing, creating a 'lock-in' response in the shear layer. In all instances, there is clear evidence that the flush transverse jet's near-field shear layer becomes globally unstable when R lies at or below a critical range near 3. These findings have important implications for and provide the underlying strategy by which active control of the transverse jet may be developed.

Key words: absolute/convective instability, jets, shear layers

1. Introduction

The transverse jet or jet injected into crossflow is a canonical flow field whose ubiquitous applications in engineering systems (Margason 1993) have led to extensive fundamental experimental explorations (Kamotani & Greber 1972; Moussa, Trischka & Eskinazi 1977; Broadwell & Breidenthal 1984; Fric & Roshko 1994; Kelso, Lim & Perry 1996; Smith & Mungal 1998) as well as theoretical and computational studies (Karagozian 1986; Yuan & Street 1998; Cortelezzi & Karagozian 2001; Muppidi & Mahesh 2007). The jet-in-crossflow (JICF) typically consists of a round jet of mean velocity U_j issuing perpendicularly into a crossflow of velocity U_∞, with the jet exiting either flush from an orifice embedded within a wall, as shown in figure 1, or from an elevated pipe or nozzle. The transverse jet interacts in a complicated three-dimensional manner with the crossflow and, for the case of the flush jet in crossflow, with the injection wall boundary layer. The fundamental dynamics of the JICF involve an inter-related set of vortex systems, including upstream shear-layer vortices, the counter-rotating vortex pair (CVP) observed to dominate the jet cross-section (Kamotani & Greber 1972; Smith & Mungal 1998), horseshoe vortices which form in the plane of the flush jet's injection wall (Kelso & Smits 1995) and upright wake vortices (Fric & Roshko 1994). Among the non-dimensional parameters used

† Email address for correspondence: ark@seas.ucla.edu

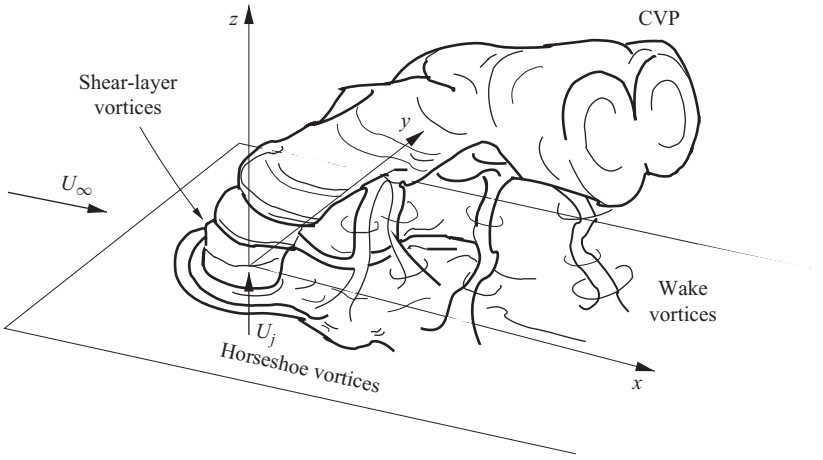

FIGURE 1. Schematic of the transverse jet, introduced flush with respect to the injection wall, and relevant vortical structures and axes. Crossflow U_∞ is in the positive x direction. Adapted from Fric & Roshko (1994).

to characterize this isodensity flow field are the mean jet-to-crossflow velocity ratio R and the jet Reynolds number Re, which is based on the jet's inner diameter D and mean jet velocity U_j.

Because the formation of the CVP is known to be associated with mixing enhancement and is thought to be influenced by the transverse jet's shear-layer vortices (Kelso *et al.* 1996; Cortelezzi & Karagozian 2001), it has been of interest to understand the nature of the jet's upstream shear-layer instabilities. A number of experimental studies indicate that the shear-layer vortices result from a Kelvin–Helmholtz instability near the jet exit (Kelso *et al.* 1996; Yuan & Street 1998). Recent numerical simulations (Alves 2006; Bagheri *et al.* 2009) suggest that the CVP actually has an axisymmetric steady component and a non-axisymmetric unsteady component arising from the Kelvin–Helmholtz instability associated with the shear layer. Yet a few previous studies indicate that at relatively low jet-to-crossflow velocity ratios, below the range of $R = 3$–4, the onset of the shear-layer instability is driven by mechanisms which may be different from the typical Kelvin–Helmholtz instability, in that there is a very strong oscillation or 'waving' in the flow (Camussi, Guj & Stella 2002), leading to 'large scale, periodic' shear-layer roll-up (Kelso *et al.* 1996).

Changes in the transverse jet's shear-layer instabilities with respect to jet-to-crossflow velocity ratio R have been recently explored in both experimental and theoretical studies. Gas-phase experiments incorporating both flush and elevated jets in crossflow (Megerian *et al.* 2007) in the range $\infty < R \leqslant 1.15$ indicate that the nature of the transverse-jet shear-layer instability can be significantly different from that of the free jet, and that the instability changes in character as R is reduced to below approximately 3.5. In contrast to the free jet's relatively weak fundamental instability and spatial evolution of a lower frequency preferred mode (Ho & Huerre 1984), the transverse-jet shear-layer instabilities occur closer to the jet exit as crossflow velocity increases, with exhibition of frequency-shifting or 'hopping' from lower to higher frequencies as one moves downstream along the jet shear layer for both flush and elevated nozzle configurations at moderately high values of R. Linear stability analysis (LSA) of the transverse-jet shear layer for relatively large velocity ratios, $R > 4$ (Alves, Kelly & Karagozian 2008) predict variations in Strouhal number and in growth rates

of the instabilities with variable R that compare well with experimental measurements for the flush jet in this regime. For both theory and experiments, Strouhal number ($St \equiv f_o D/U_j$) is based on f_o, the frequency of the initial fundamental instability that is observed to develop along the jet shear layer.

In the flush injection experiments, when R is reduced below around 3.5, single-frequency instabilities are dramatically strengthened, forming closer to the jet exit with decreasing R. There are also higher harmonics present in such shear-layer spectra, with no evidence of frequency shifting. When the value of R falls below approximately 2.5, there is little evidence of the formation of subharmonics, only very strong fundamental and somewhat weaker higher harmonics. Similar behaviour is observed in the elevated jet, except that the transition to the generation of strong modes occurs at a lower value of R (around 1.2) due to the influence of vertical coflow exterior to the elevated nozzle in weakening the instabilities (Megerian *et al.* 2007). In addition to these alterations in the spectral character of the transverse-jet upstream shear layer, very low level forcing of the jet at frequencies $f_f \neq f_o$ (with amplitudes less than one percent of the mean jet velocity) has no appreciable influence on the shear-layer response when the strong modes are present at lower R values. In contrast, for jets at higher R values, when very low level jet excitation is imposed, the forcing frequency dominates the shear-layer spectra.

This significantly altered behaviour in the transverse jet as R is reduced below a critical regime (Megerian *et al.* 2007) suggests a possible transition in the upstream shear layer from being convectively unstable at higher jet-to-crossflow velocity ratios to becoming self-sustained or globally unstable at lower values of R. While the LSA by Alves *et al.* (2008) could not detect such a transition due to its validity for higher velocity ratios only ($R \gtrsim 4$), separate evidence for this transition is available in the recent direct numerical simulations (DNS) and LSA by Bagheri *et al.* (2009). These studies suggest that the flow is 'globally linearly unstable' at the single condition examined in the simulations, $R = 3$. In the experiments (Megerian *et al.* 2007), an exponential growth rate for the disturbances is still detected near the transition condition (at $R \approx 3$), so LSA is an accurate technique for detecting this type of transition to global instability. Large eddy simulations of the round JICF by Ziefle & Kleiser (2009) for a low velocity ratio (3.3) and with fully developed turbulent pipe flow at the jet exit show qualitatively similar shear-layer instabilities to those in Megerian *et al.* (2007).

The presence of global instability in a number of different types of shear flows is well known (Huerre & Monkewitz 1990). As noted by Chomaz (2005), evidence in the spatial evolution of the disturbance amplitude for a nonlinear global mode in an infinite domain consists of a sharp front located at the upstream boundary of the absolute instability region, where the disturbance amplitude abruptly increases and stays high as one moves downstream. Under such conditions the flow behaves as an oscillator rather than a noise amplifier. Flows that can become globally unstable include low-density axisymmetric jets in quiescent surroundings below a critical jet-to-surroundings density ratio (Monkewitz *et al.* 1990; Kyle & Sreenivasan 1993), countercurrent mixing layers above a critical velocity difference (Strykowski & Niccum 1991, 1992) and wake flows above a critical Reynolds number (Provansal, Mathis & Boyer 1987; Hammond & Redekopp 1997). The evidence for such transitions includes phenomena that already have been documented in Megerian *et al.* (2007) for the transverse jet, e.g. (i) clear changes in the spectral character of the shear layer, with strong oscillations at narrow spectral peaks for global instability, representing pure tones with higher harmonics, (ii) a rather dramatic alteration in the value of the Strouhal number associated with the initial instability as the influencing

flow parameter is brought into the range for globally unstable flow and (iii) little spectral alteration of the globally unstable flow in response to low to moderate flow excitation, in contrast to significant spectral alteration of the convectively unstable flow during such excitation. Additional phenomena associated with a transition to globally unstable conditions include: (iv) a rather abrupt increase in the amplitude of the disturbance within and near the shear layer as one approaches the critical flow parameter, consistent with the characteristics of the Landau equation (Huerre & Monkewitz 1990; Strykowski & Niccum 1991) and (v) a reduction in the energy transfer from fundamental to subharmonic frequencies along the shear layer, and hence a reduction in the strength of subharmonics and corresponding inhibition of the vortex pairing process after the transition. In addition, for the low-density free jet it has been shown that very strong external sinusoidal excitation can be used to overcome the fundamental instability mode for globally unstable conditions (Hallberg & Strykowski 2008; Juniper, Li & Nichols 2009). These findings are consistent with the theoretical work of Pier (2003), which suggests that for spatially developing flows, external forcing upstream of the transition from convective to absolute instability can overwhelm the naturally occurring absolute instability. The low-density jet experiments show that at forcing frequencies f_f that are relatively close to the global instability frequency, f_o, and/or at very high-amplitude forcing, the global frequency is not observed at all, and the forcing frequency dominates the flow's spectral character, with the capacity to either reduce or enhance jet mixing. The excitation amplitude at which the flow 'locks' on to the forcing frequency f_f increases in proportion to $|f_o - f_f|$, consistent with the flow transition to a global mode via a Hopf bifurcation (Huerre & Monkewitz 1990; Chomaz 2005). The capacity for strong sinusoidal forcing to alter the global instability is viewed as a means of controlling the low-density jet.

It is of interest in the present experimental study to explore the transverse-jet shear-layer transition observed in Megerian *et al.* (2007) in greater detail, not only providing additional evidence for this transition to globally unstable flow, but also to understand the specific phenomena associated with this transition and the critical conditions under which it occurs. If indeed the transverse-jet shear layer becomes globally unstable below a critical jet-to-crossflow velocity ratio, this could have important implications for the ability to control the jet via external excitation (M'Closkey *et al.* 2002; Shapiro *et al.* 2006). It is with this application in mind that the present exploration of the instabilties has been conducted.

2. Experimental set-up

Figure 2 provides a schematic diagram of the present experimental set-up, which is the same as that used and described in Megerian *et al.* (2007) and in greater detail in Davitian (2008). A nitrogen jet issued perpendicularly into the crossflow of air at room temperature, which was introduced by a compressor into the wind tunnel. Crossflow speeds upstream of the jet ranged from 1.3 to 7.2 m s^{-1}, with turbulence intensities less than 1.5 %. In these prior experiments, two alternative round-jet nozzles were utilized, one oriented flush with respect to the bottom tunnel wall and one with its exit plane extending from the injection wall into the tunnel, but otherwise they were identical in shape. The nozzles were formed with a fifth-order polynomial contraction and an inner diameter at the nozzle exit of 3.81 mm, with the same nozzle length and distance between the gas inlets and nozzle exit plane. As noted previously, the stability characteristics of the transverse jets formed by these two nozzles are generally

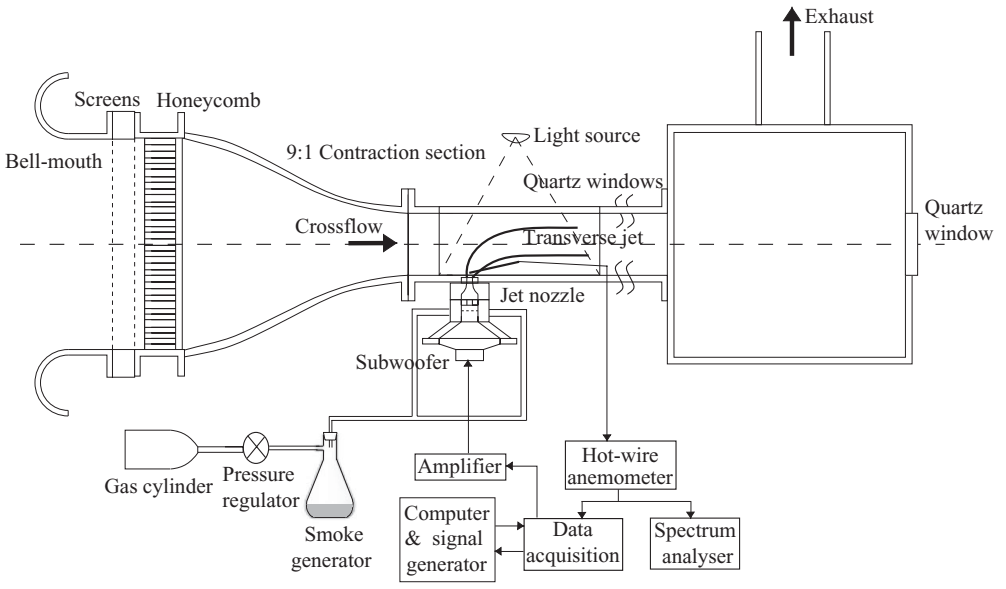

FIGURE 2. Schematic diagram of the low-speed wind tunnel and associated transverse-jet nozzle and excitation apparatus, where excitation was used only for sinusoidal forcing in the present experiments. The actual tunnel had three additional sections situated downstream of the one shown, of identical dimensions.

similar, only with different values or ranges of R below which the transition in the instabilities takes place, due to the effects of coflow for the elevated nozzle. This paper has a focus on only the flush nozzle.

Excitation in these and prior experiments (Shapiro *et al.* 2006; Megerian *et al.* 2007) was accomplished through a loudspeaker placed at the bottom of a plenum assembly attached to the nozzle. The desired temporal input signal (sinusoidal in the present experiments) was generated using the Matlab 6.5 Simulink program and delivered to the amplifier via a dSPACE acquisition board.

The present studies focused on a fixed jet exit velocity, producing $Re = 2000$; prior studies demonstrate that very similar instability characteristics are observed for larger Reynolds numbers ($Re = 3000$) at the same jet-to-crossflow velocity ratio, R. The converging nozzle was designed to achieve a nearly top hat velocity profile at the exit plane, with a relatively small jet momentum thickness. As documented in Megerian *et al.* (2007), the exit velocity profiles of the two nozzles are symmetric and virtually identical for the same Reynolds numbers and jet-to-crossflow velocity ratios from $R \rightarrow \infty$ down to about $R \approx 4$, below which clearer asymmetries in the exit profile begin to develop and the upstream shear layer becomes thicker than the downstream shear layer. A single component hot-wire anemometer (Dantec 55P15) was used in these studies to quantify the spectral character of the vertical disturbance velocities within and in the vicinity of the jet shear layer. The hot wire was connected to a Dantec Dynamics StreamLine 90N10 frame, with the probe attached to three Newport high-performance low-profile ball bearing linear stages, creating a triple axis manual traversing platform with a spatial accuracy of 1 μm (2.6×10^{-4} jet diameters). Details on signal analysis and processing are documented in Megerian *et al.* (2007) and Davitian (2008).

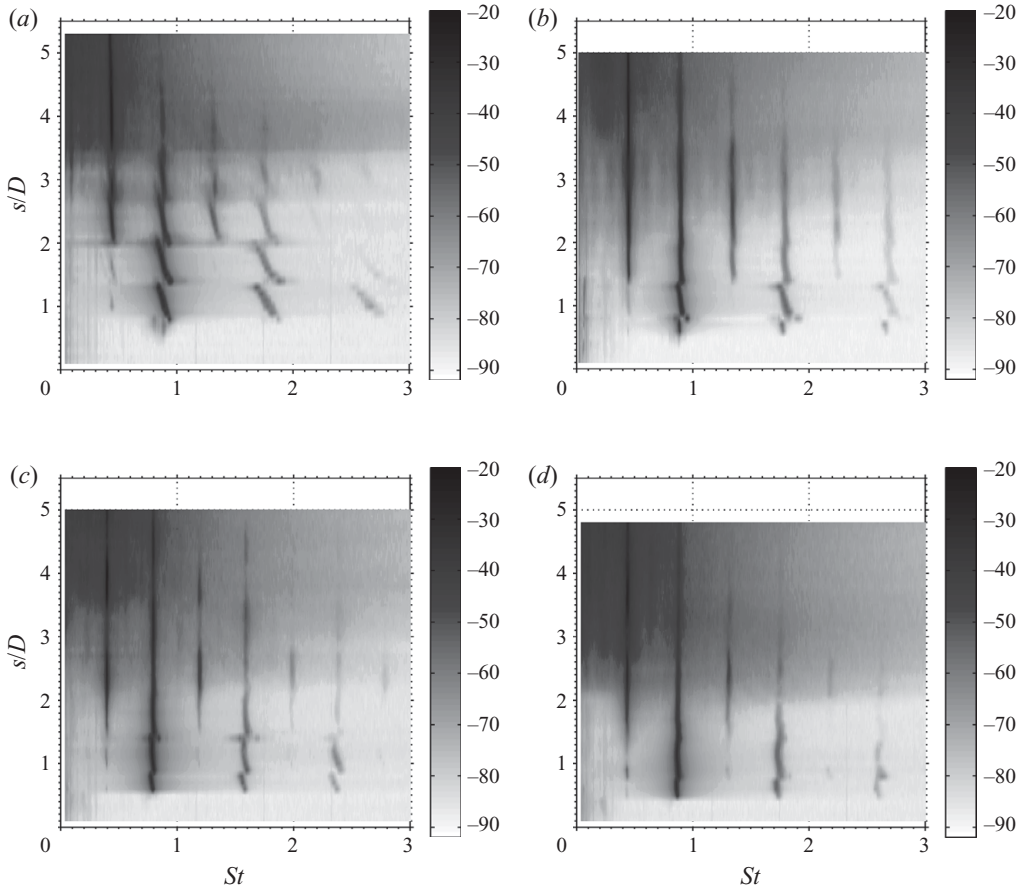

FIGURE 3. Contour plots of the disturbance amplitude measured by the hot wire along the upstream shear layer (s/D variable) for the flush transverse jet at jet-to-crossflow velocity ratios $R = 3.50$ (a), 3.35 (b), 3.25 (c) and 3.00 (d). Frequencies (shown as Strouhal number) are indicated on the abscissa, and the grey scale (in dB) represents disturbance amplitude.

3. Results

3.1. *Instabilities in the upstream shear layer*

Results for the spectral behaviour of the evolution of the upstream shear layer for the transverse jet are shown in detail in Megerian *et al.* (2007) for fixed jet Reynolds numbers of 2000 and 3000. The trajectory of the upstream shear layer was determined by maxima in the velocity gradient across the jet, and this was done in the present experiments as well. Alterations in the natural (unforced) transverse-jet shear-layer instability for various jet-to-crossflow velocity ratios R may be summarized in contour plots indicating the magnitude of the local instability at various non-dimensional locations s/D, measured from the jet exit along the jet's upstream shear layer. Such contour plots are shown closer to the transitional behaviour, for example, in figure 3, with the abscissa indicating Strouhal numbers associated with the local instabilities. In the figures here, R ranges from 3.5 down to 3.0, which is achieved by increasing crossflow with a fixed jet Reynolds number ($Re = 2000$).

The contour plots in these figures indicate clear differences in the shear-layer spectral character for different values of R. In figure 3(a) for the flush jet at $R = 3.50$, which

had been previously supposed to be close to the start of absolutely unstable behaviour (Megerian *et al.* 2007), the instabilities were initiated closer to the jet exit than for higher R values, but still with frequency shifting and sudden 'hopping' to higher frequencies as the probe was moved along the upstream shear layer. This unusual frequency shifting behaviour is documented for all transverse jets at jet-to-crossflow velocities exceeding 3.5, up to 10, in Megerian *et al.* (2007) and Davitian (2008). Formation of a subharmonic further downstream was typically observed at these higher R values, as is observed for the convectively unstable free jet (Ho & Huerre 1984). Higher harmonics with similar frequency shifting were also observed for the transverse jet, e.g. as in figure 3(*a*). In contrast, as crossflow velocity was increased and R reduced (figures 3*b*–3*d*), the extent of frequency shifting diminished, and eventually there was initiation of a strong dominant mode that persisted along the shear layer. For the contour plots shown here with $R \geqslant 3.0$, subharmonic disturbances as well as higher harmonics also formed beyond the jet exit, but as indicated in Megerian *et al.* (2007) and as will be described in detail below, when R was reduced, subharmonic disturbances were significantly weakened.

The changes in the spectral character observed here, as well as the visible features of the transverse jet's upstream shear layer with decreasing jet-to-crossflow velocity ratio R, seen via smoke visualization in Davitian (2008), suggested a transition from a convectively unstable flow at higher R to an absolutely unstable flow at lower R, where very strong disturbances formed close to the initiation of the shear layer, as observed in other flows known to exhibit globally unstable characteristics (Huerre & Monkewitz 1990; Chomaz 2005). Yet the results in figure 3 suggest that the critical jet-to-crossflow velocity ratio at which this transition occurs may not be $R_{cr} \approx 3.5$, as had been previously estimated, but in fact lies at a somewhat lower R value. To explore these instabilities in greater detail, changes in the spectra very close to the jet exit, at fixed relative locations s/D along the upstream shear layer, were explored at small decrements in R. This approach is similar to the exploration of countercurrent mixing layers with varying velocity ratios by Strykowski & Niccum (1991), where strong energetic oscillations at a discrete frequency and a two order of magnitude increase in the root-mean-square (r.m.s.) of the velocity perturbations just above the critical velocity ratio are observed. In the case of the transverse jet, vertical velocity spectra and corresponding time-series data were acquired for fixed s locations along the shear-layer trajectory for successively decreasing values of R.

For example, spectra as well as time-series data measured at a distance $s/D = 0.7$ along the shear layer, as R was decreased from 3.4 to 3.1 for the flush jet, are shown in figure 4, providing data on the initiation of the instabilities. It should be noted that, due to the alteration in the jet trajectory with varying R, the fixed s/D position here did not correspond to fixed x and z values in the flow field. As R was reduced, there was a gradual strengthening of a single mode near $St = 0.8$, so that at $R = 3.1$, the spectral peak became relatively narrow, and the r.m.s. amplitude of the velocity oscillations increased substantially. Similar behaviour was observed for the elevated transverse jet (Davitian 2008), but with the large increase in oscillations occurring at $R = 1.20$.

Information such as that provided in figure 4 could suggest that the critical velocity ratio at which the flush jet transitioned to global instability was at or close to $R = 3.1$. Yet as noted in Strykowski & Niccum (1991), different fixed spatial locations along a shear layer could produce different values of the critical parameter at which the transition to global instability occurs. Data at different spatial locations are in fact used by Strykowski & Niccum (1991) to suggest whether the bifurcation occurring

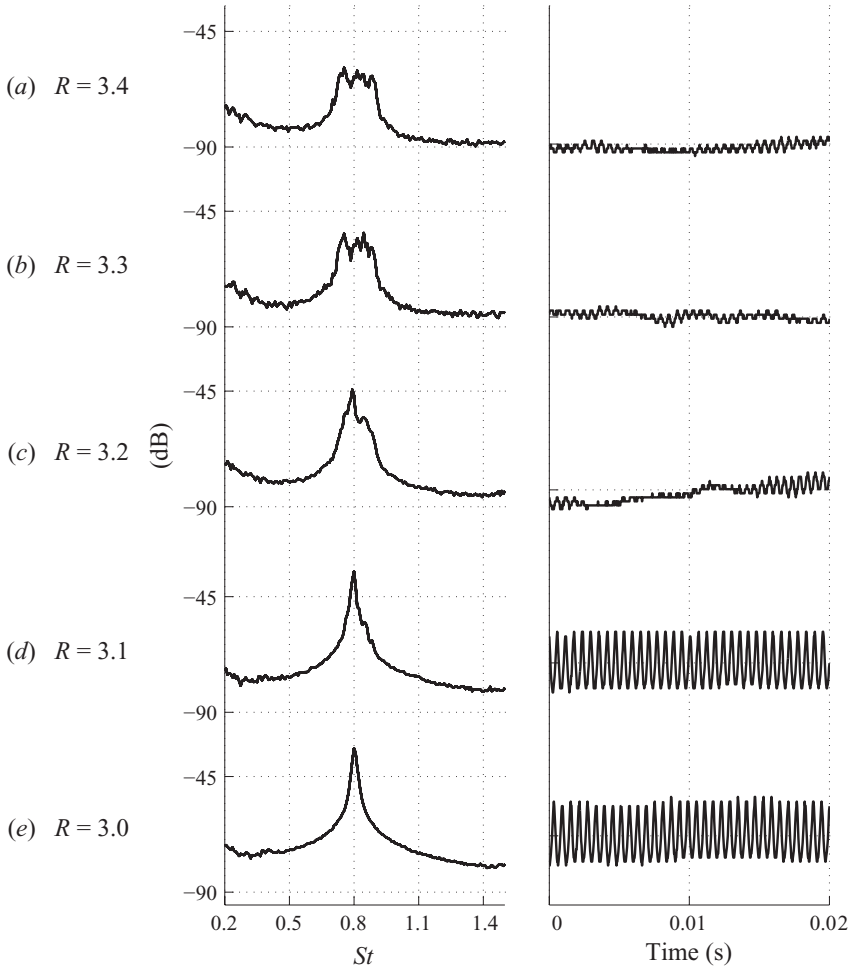

FIGURE 4. Evolution of upstream shear-layer velocity spectra (left) and corresponding time-series oscillations (right) for the flush transverse jet at $s/D = 0.7$, for $3.4 \geqslant R \geqslant 3.0$. The time-series measurements are scaled identically on the ordinate axis.

at their critical velocity ratio (for the countercurrent mixing layer) might be of the supercritical Hopf type. Under such conditions, these researchers find that features of the instability may be modelled by the Landau equation (Huerre & Monkewitz 1990; Chomaz 2005), where the disturbance amplitude of the global oscillations in the limit of zero forcing of the system scales in proportion to the square root of the difference between the flow parameter and its 'critical' value. This feature was explored for the transverse jet.

As done by Strykowski & Niccum (1991) for the countercurrent mixing layer, in the present transverse-jet experiments the hot wire was positioned in the shear layer of the jet at a fixed location s/D and velocity ratio R was varied for the fixed Reynolds number. Recordings of the r.m.s. amplitude of the velocity fluctuations (scaled by mean jet velocity) for three different s/D values (0.1, 0.5 and 1.0) are plotted in figure 5. As R was systematically reduced, significant increases in the square of the disturbance amplitude $(u'_{rms}/U_j)^2$ at the fixed shear-layer location s/D were observed. As noted in Strykowski & Niccum (1991), one can extrapolate the

s/D location	R_{cr} (linear fit)	R_{cr} (contour)
0.1	1.8	2.8
0.5	2.9	3.2
1.0	4.3	4.7

TABLE 1. Approximate values of critical jet-to-crossflow velocity ratios at which one could predict the start of absolutely unstable flow based on disturbance measurements at different locations along the upstream shear layer, s/D. R_{cr} (linear fit) is obtained from the linear extrapolations shown in figure 5, and R_{cr} (contour) is obtained from the data in figure 6.

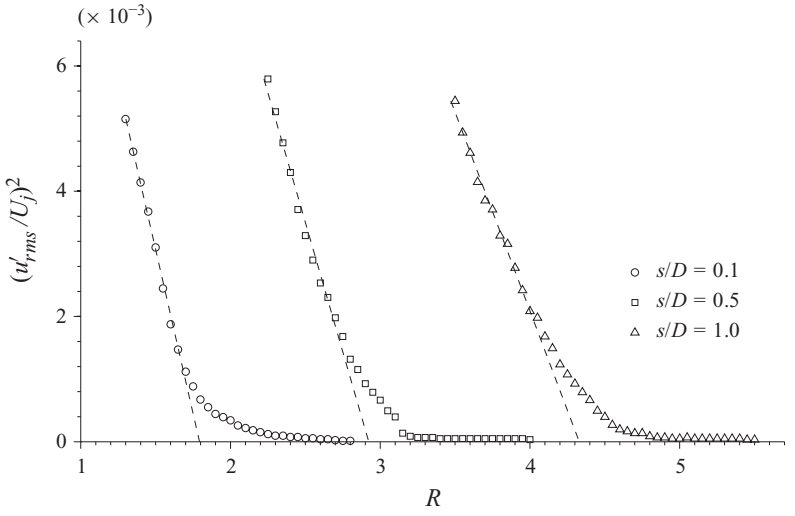

FIGURE 5. The saturation amplitude of velocity perturbation in the shear layer, scaled by mean jet velocity and measured at fixed spatial locations $s/D = 0.1$, 0.5 and 1.0, for a range of jet-to-crossflow velocity ratios R. The linear relationship between $(u'_{rms}/U_j)^2$ and R can be extrapolated to locate the critical R value at $u'_{rms} = 0$.

linear amplitude dependence in figure 5 as one means of predicting a critical velocity ratio, R_{cr}, beyond which the global instability dominates. This is indicated by the straight line extrapolations in the figure. The linear extrapolations for $s/D = 0.1$, 0.5 and 1.0 yield different estimates for the critical velocity ratio, R_{cr}, as shown in table 1. Such differences in the critical flow parameter (dependent on probe location) are also observed and quantified for the countercurrent shear layer. Since the total spatial amplification of disturbances in the transverse-jet shear layer increases along the jet, as with other flows that become globally unstable, there may be larger errors in the estimate of R_{cr} when measurements are made at larger values of s/D, as noted by Strykowski & Niccum (1991) for counterflow jets.

Additional details on the initiation of these instabilities at fixed relative locations s/D along the shear layer may be observed in contour plots showing the disturbance frequency (in terms of Strouhal number St) and disturbance amplitude in dB for different R conditions. These are shown in figure 6(a–c) for $s/D = 0.1$, 0.5 and 1.0. The critical R value at which the amplitude of the fundamental disturbance becomes visibly larger for these three spatial locations differs from that estimated from the linear extrapolation in figure 5; these values are also shown in table 1.

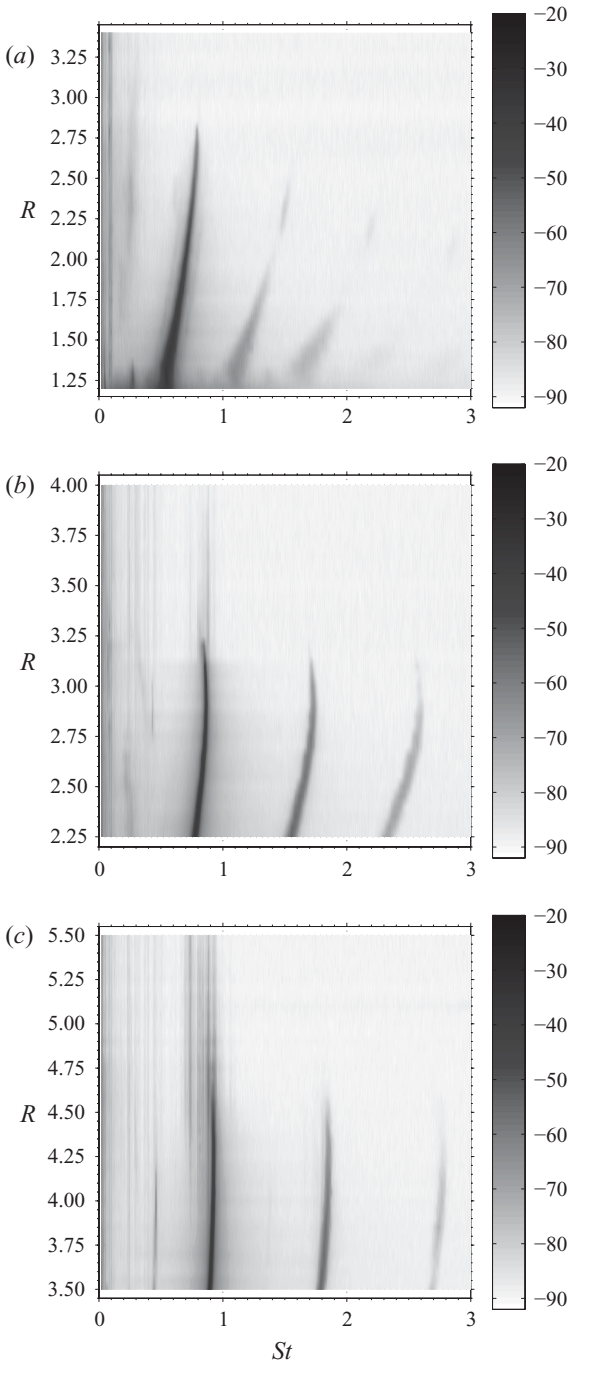

FIGURE 6. Contour plots of the disturbance amplitude measured by the hot wire at a fixed location s/D along the transverse-jet shear layer for different jet-to-crossflow velocity ratios R ($s/D = 0.1$ (*a*), 0.5 (*b*) and 1.0 (*c*)). Frequencies of the disturbances (written in terms of Strouhal number) are shown on the abscissa and the grey scale (in dB) represents disturbance amplitude.

Hence there are a number of alternative approaches for determining the critical velocity ratio R_{cr} at which the transverse-jet shear layer begins to exhibit globally unstable behaviour, shown in figures 3–6. Taken in total, and building on the approaches used previously for such characterizations for other globally unstable flows, the present data suggested that R_{cr} values in the range of 3.0–3.3 were likely to be the most accurate estimate of the transition regime, especially given that transverse-jet shear layers at $R \approx 3$ and at Reynolds numbers of either 2000 or 3000 do not respond to any significant extent to low-level external excitation (Davitian 2008). The whole shear-layer instability contour maps as shown in figure 3 may be the most appropriate determination of whether or not the jet has become absolutely unstable, based on the distinctive visual differences between transverse jets at higher velocity ratios R with frequency shifting behaviour (e.g. as in figure 3*a*), and those with strong disturbances that are relatively unaltered downstream (e.g. as in figure 3*d*).

3.2. *Energy transfer to subharmonic frequencies*

As noted previously, another known indication for a transition from convective to absolute instability involves a significant reduction in the energy transfer from fundamental to subharmonic modes along the shear layer, and hence a reduction in the strength of subharmonics after the transition has taken place. For example, in experimental studies of countercurrent jet mixing layers, Strykowski & Niccum (1992) observe that in the convectively unstable regime, the fundamental instability is suppressed along the jet after saturation due to an energy transfer from this frequency to the subharmonic, but once the shear layer is globally unstable, the energy transfer from fundamental to subharmonic is inhibited.

This same transfer mechanism was examined for the transverse jet at velocity ratios above and below the transition observed in the R regime of 3.0–3.3. Spatial growth of the fundamental and the subharmonic modes was explored along the upstream shear layer, for example, for the $R = 3.5$ condition just before transition, and for $R = 2.5$, after the transition took place. These results for the amplitude of the disturbances along the jet, as well as corresponding contour plots representing the spatial evolution of all disturbances, are shown in figure 7. Tracking of the frequency bands associated with the fundamental and subharmonics was aided by contour plots such as those in figure 7(*c*, *d*). For $R = 3.50$, as previously noted, there was typically frequency shifting and hopping within a broader range of frequencies for the fundamental as one moved along the jet shear layer, hence a wider band of frequencies was tracked as the 'fundamental' than for the rather narrow fundamental frequency band for $R = 2.5$, indicated in figure 7(*d*).

For the higher R case, i.e. figure 7(*a*), there was evidence of an exponential growth in the amplitude of the fundamental disturbance within one diameter of the jet exit, but after two diameters, the magnitude of the subharmonic disturbance grew substantially, with a drop-off in that for the fundamental. The energy transfer from the fundamental to the subharmonic was thus clearly evident by about two diameters along the upstream jet shear layer. In contrast, for $R = 2.5$, shown in figure 7(*b*), the fundamental grew exponentially immediately beyond the jet exit until approximately $s/D = 0.5$. Although a subharmonic disturbance was evident, it was quite weak. The fundamental did not saturate, nor was there energy transfer from the fundamental to the subharmonic for this condition. This behaviour provided additional compelling evidence for the transition to globally unstable flow conditions when R was brought below its critical range.

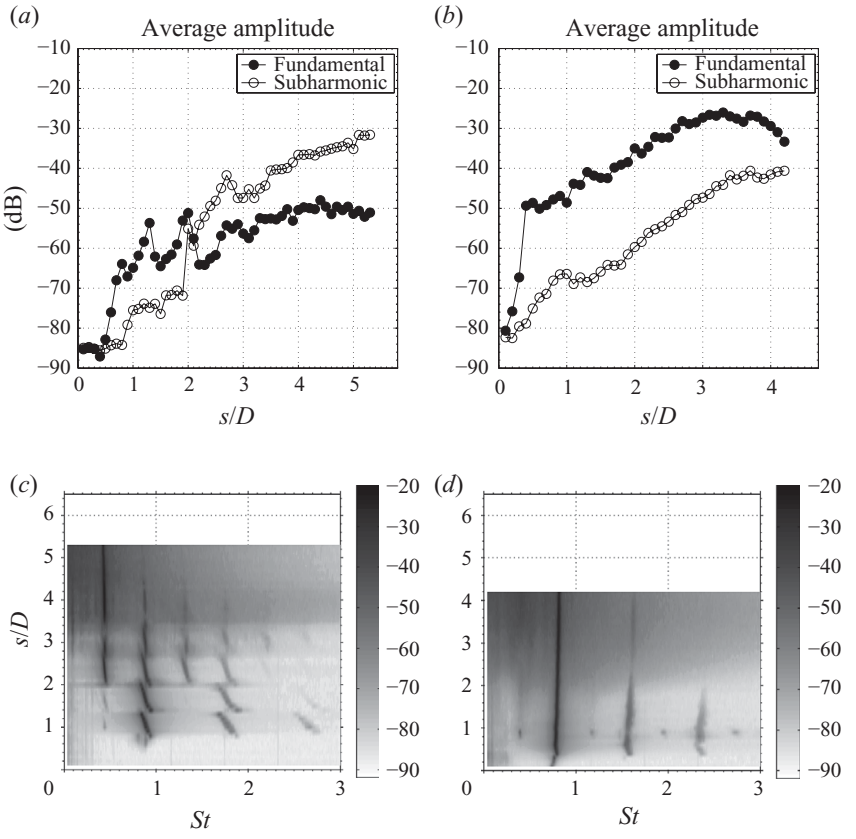

FIGURE 7. Development of the fundamental and subharmonic modes in the flush transverse jet's upstream shear layer for (*a*) $R = 3.5$ and (*b*) $R = 2.5$. Corresponding contour plots are shown in (*c*) and (*d*), respectively.

3.3. *Development of instabilities about the jet periphery*

Many of these dramatic alterations in the nature of the upstream shear-layer instabilities raise the issue of the spatial variation in the disturbances. The linear stability analysis for the transverse jet with a continuous base flow by Alves *et al.* (2008) suggests that the nominally axisymmetric mode is the most unstable disturbance for the case of larger R values, with good quantitative comparison of Strouhal numbers and growth rates with the experiments in Megerian *et al.* (2007). A uniformly valid asymptotic expansion analysis for the transverse jet with $R \gg 1$, described in Kelly & Alves (2008), shows that the shear flow giving rise to instabilities in the transverse jet occurs due to both axial jet flow and circumferential flow about the jet arising from the crossflow. Hence the transverse jet provides an opportunity to study the transition to global instability in a fully three-dimensional flow field. Furthermore, the transverse-jet linear stability analysis performed by Alves, Kelly & Karagozian (2007) with an irrotational base flow shows that, for low Strouhal numbers, helical modes with different signs have different spatial growth rates for $R > 3$. These asymmetries are suggested to be responsible for the asymmetries observed in the mean CVP profile observed experimentally (Kuzo 1995; Smith & Mungal 1998). Hence in the present studies it was of interest to explore the variation in instabilities around the periphery of the evolving jet to ascertain its role in the generation of disturbances.

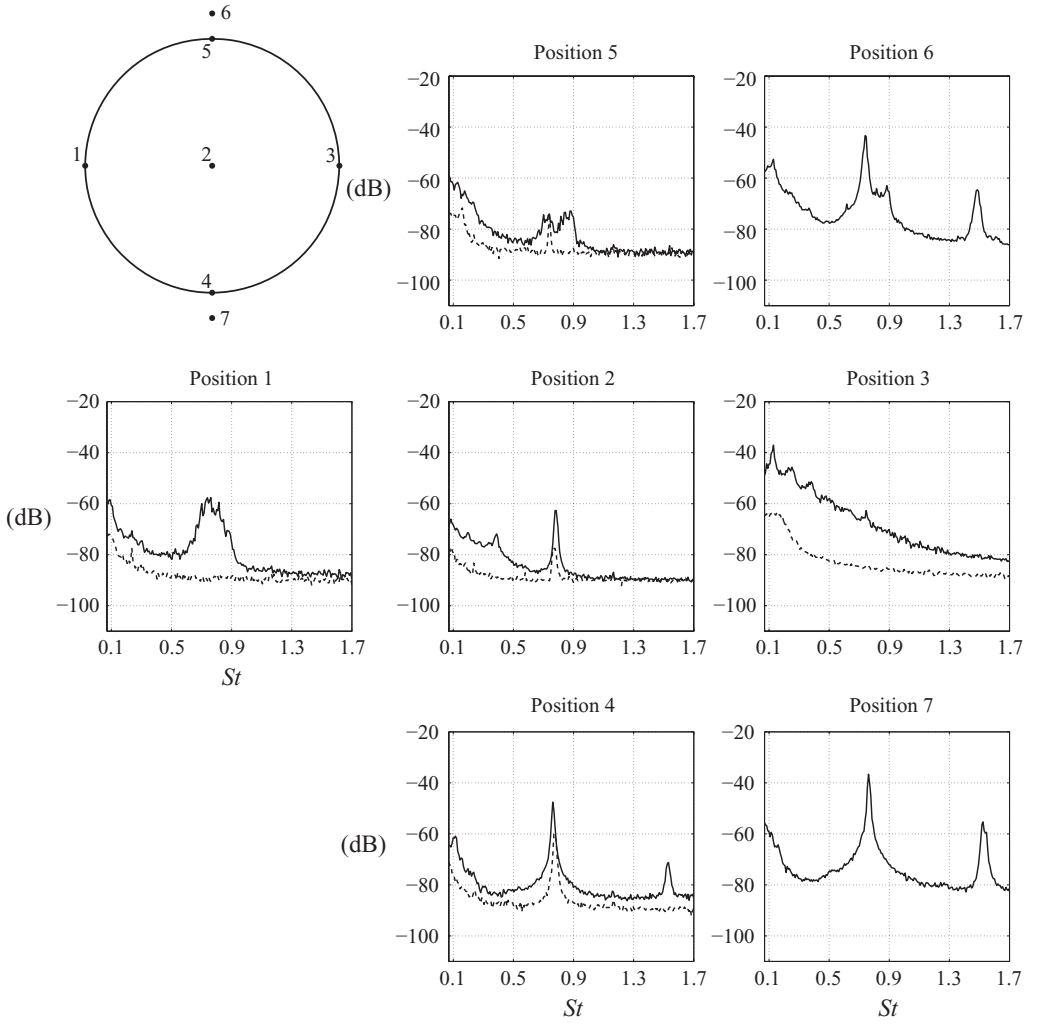

FIGURE 8. Vertical velocity spectra for the flush transverse jet at different positions around the jet (as shown in the inset, with crossflow from left to right) for $R = 3.3$. Spectra are shown for different elevations along the jet ($s/D = 0.1$ is dashed and $s/D = 0.7$ is solid).

Vertical velocity spectra were acquired for a range of R values near and below the critical range $R \approx 3.0$–3.3, at various positions about the edge of the flush jet along its near-field trajectory. Sample results for spectra measured about the transverse jet for $R = 3.3$, 3.0 and 1.15 are shown in figures 8, 9 and 10, respectively. The locations of the measurements relative to the orifice (when s/D is small) are shown in each figure, with numbered positions at the centre (2) and periphery (1, 4, 3 and 5) of the jet, as well as positions one-tenth of a diameter from the edge of the orifice in the spanwise direction (positions 6 and 7). At measurement locations further along the jet trajectory (for $s/D > 0.1$), position 1 corresponded to the location of the upstream shear layer of the deflected jet (locus of maximum velocity gradient), with the other spatial positions located relative to 1.

While at $R = 3.3$ the upstream shear-layer spectrum near the jet orifice (at position 1 and at $s/D = 0.7$) did not have a very strong peak, as indicated in figure 8, it

is interesting to note that under these flow conditions a single mode of moderate amplitude appeared at the centre of the jet, with a stronger one at the same frequency, near $St \approx 0.8$, at the side of the jet with negative y (positions 4 and 7). In contrast, there were very weak disturbances on the other side of the jet for $y > 0$ (position 5), although there was some strengthening of the instability just outside of the jet periphery, seen at position 6. At position 3, near the wake of the jet, higher amplitude, lower frequency disturbances with a decay in the strength of the disturbances at higher frequencies was observed, consistent with typical wake characteristics. The hot-wire probe entered the test section from the positive y side of the experiment, that is, from the side where positions 5 and 6 are located, hence for the measurements made at these locations, the hot-wire apparatus could have blocked the effect of the crossflow and thus only measured the flow adjacent to the jet at positions 5 and 6, whereas at positions 4 and 7, the hot wire measured the flow at the edge of the jet with the actual influence of the crossflow present (but with a possible blockage of some of the jet flow). Hence, while the asymmetry in the spectra shown in figure 8 may have been in part a result of the measurement technique, there was evidence of a stronger instability at the side of the jet, where the influence of shear via the circumferential flow was stronger, than at the upstream shear layer. These observations at this transitional value of R may possibly be consistent with the asymmetry in the helical mode suggested in the analysis in Alves *et al.* (2007), but the intrusive nature of the present diagnostic precluded definitive exploration of the asymmetry.

As the crossflow velocity was increased with a fixed jet Reynolds number $Re = 2000$, the instabilities detected around the evolving jet became stronger and increasingly symmetric in the y direction. When the R value was reduced to the lower limit of the transitional regime, to $R = 3.0$ in figure 9, the strong disturbance with $St \approx 0.8$ was detected about the entire jet, even in the wake region (position 3). The rather strong single-frequency disturbance for $R = 3.0$ at position 5, and hence a nearly symmetrical set of spectra about the jet orifice was testimony to the strength of the instability despite flow blockage by the hot wire. When R was reduced well below the transition, e.g. to 1.15 (figure 10), the entire flow field appeared to be dominated by the strong disturbance (now near $St \approx 0.4$), in a significantly symmetric fashion. The flow at this globally unstable condition appeared to be completely uninfluenced by any disturbance introduced by the hot wire at positions 5 or 6; in addition, there was clear detection of this instability in the wake region at position 3 in figure 10. The significant strengthening and increasingly symmetric nature of the jet's spectral characteristics at low R values could indeed be further evidence of global instability. These detailed spectral characteristics are also consistent with the visualization by Kelso *et al.* (1996) at $R < 2.3$, who state that under these conditions, 'the [jet] shear layer roll-up is of large scale, is periodic, and occurs near or within the pipe exit'.

3.4. *Response to external excitation*

Globally unstable or self-excited flows have long been demonstrated to be insensitive or weakly sensitive to external excitation, e.g. as observed for the heated or low-density jet in higher density quiescent surroundings (Sreenivasan, Raghu & Kyle 1989; Monkewitz *et al.* 1990). In contrast, a convectively unstable flow can be influenced by low-level external excitation. More recent experiments conducted by Hallberg & Strykowski (2008) and Juniper *et al.* (2009) for the globally unstable low-density round jet, building on the theoretical foundation suggested by Pier (2003), indicate that a region exists in the forcing frequency–amplitude space where the flow can be overtaken and controlled by external sinusoidal excitation that is applied well

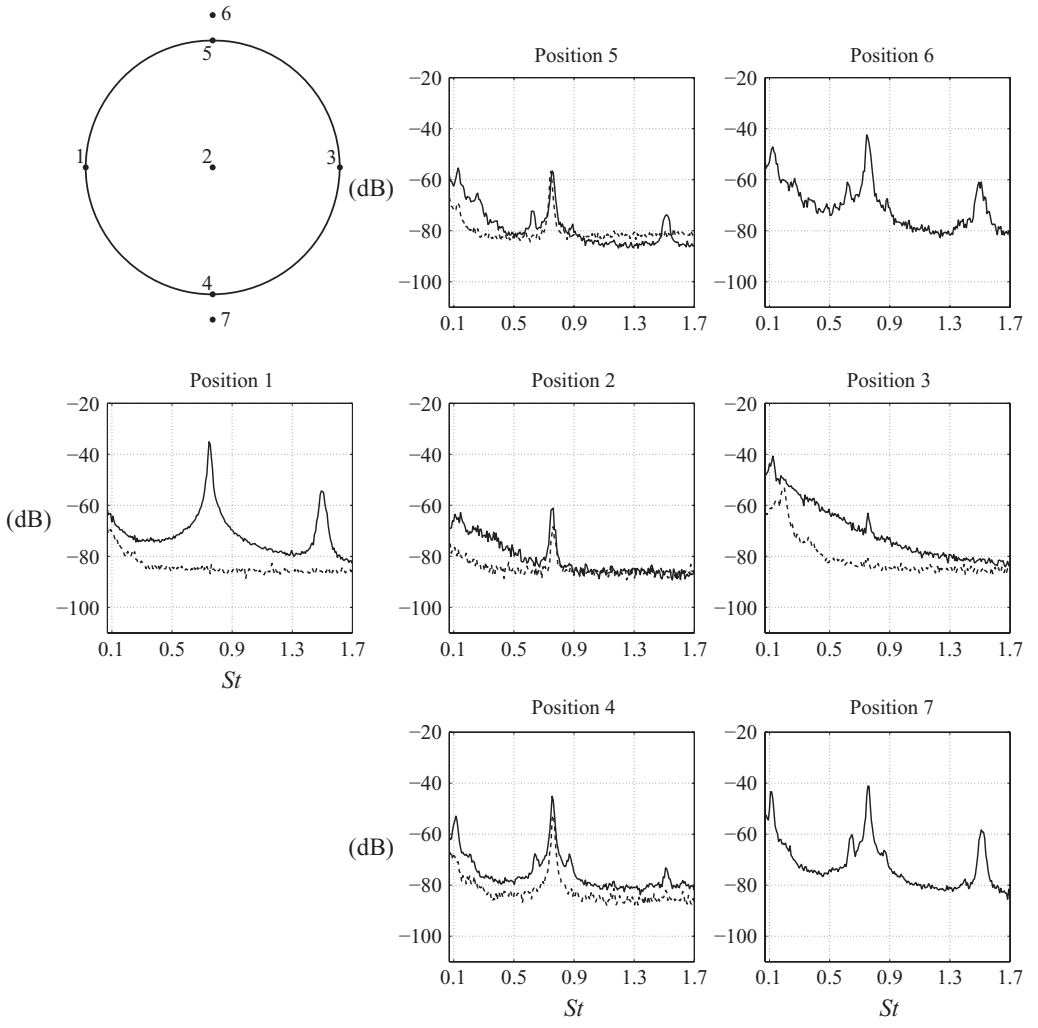

FIGURE 9. As figure 8, but for $R = 3.0$.

upstream of the location at which convectively unstable flow has become absolutely unstable. Such control can occur at a high enough amplitude of excitation and/or at forcing frequencies close to the fundamental mode, allowing for the possibility of 'open loop control' of the globally unstable jet flow.

Within the context of exploring the transition to global instability, similar experiments were conducted for the transverse jet. As noted previously, our group has documented that there is no appreciable response of the transverse jet's upstream shear layer to very low level acoustic forcing for $R \lesssim 3.5$ (Megerian *et al.* 2007), that is, for r.m.s. jet excitation velocities at the centre of the jet exit that were less than 1 % of the mean jet velocity. In these studies, sinusoidal excitation of the jet flow by the loudspeaker within the jet plenum was explored for a range of amplitudes, as high as 30 % of the mean jet velocity magnitude, and for a range of forcing frequencies f_f, with values as low as 10 % of the fundamental frequency f_o and as high as 1.6 times

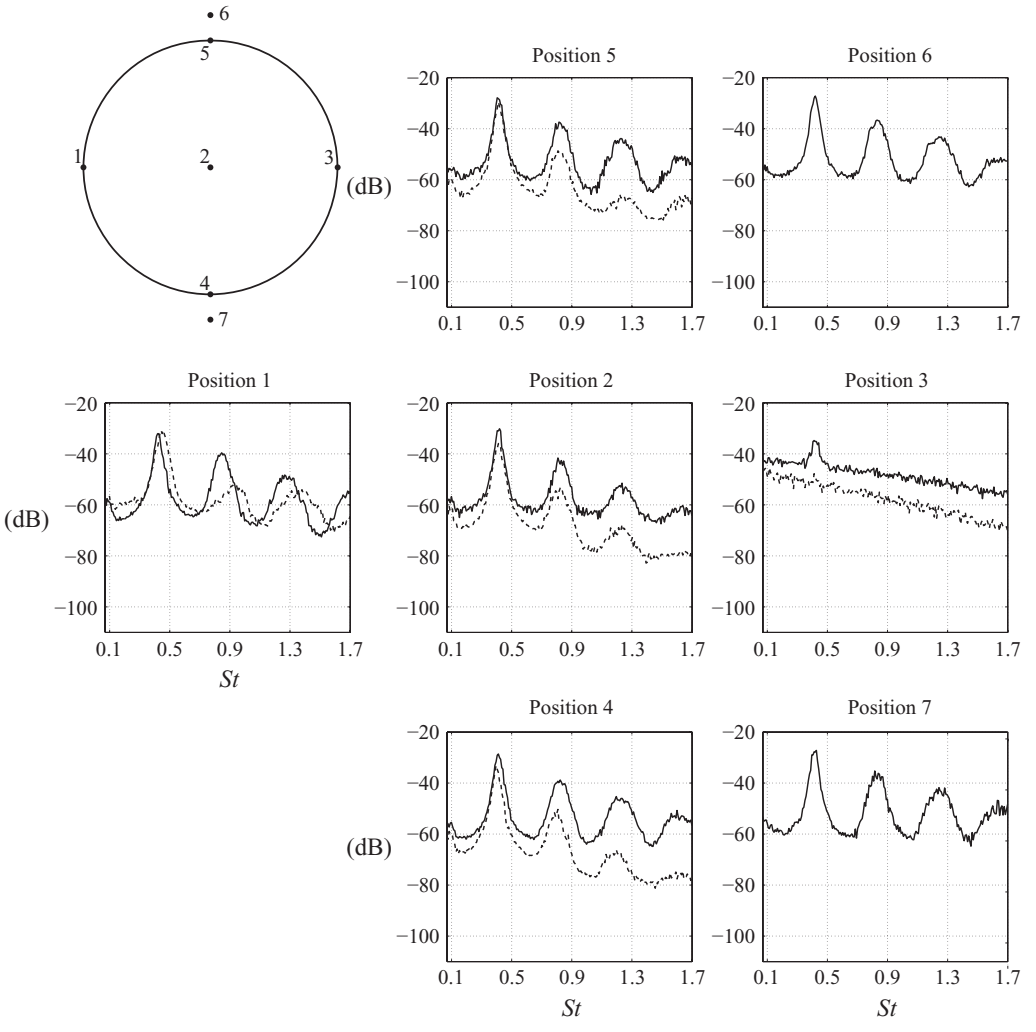

FIGURE 10. As figure 8, but for $R = 1.15$.

f_o. Limitations in the frequency response of the actuation system precluded use of excitation at significantly higher frequencies than f_o.

Observations on the response of the transverse jet's upstream shear layer to the range of excitations explored were very similar to those observed in excitation of other globally unstable flows such as the low-density free jet. For example, as shown in figure 11 for a very low jet-to-crossflow velocity ratio ($R = 1.15$) under globally unstable conditions, when the jet was excited at a very low amplitude and at a frequency other than the fundamental ($f_f = 0.6 f_o$, shown in figure 11*b*), the influence of the excitation was negligible with respect to that of the fundamental mode and the spectral characteristics were essentially identical to that for the unforced jet (figure 11*a*). When the jet was forced at certain frequencies lower or higher than that of the fundamental and at higher amplitudes (e.g. as shown in figure 11*c*), the magnitude of the shear-layer disturbance resulting from the forcing at f_f became

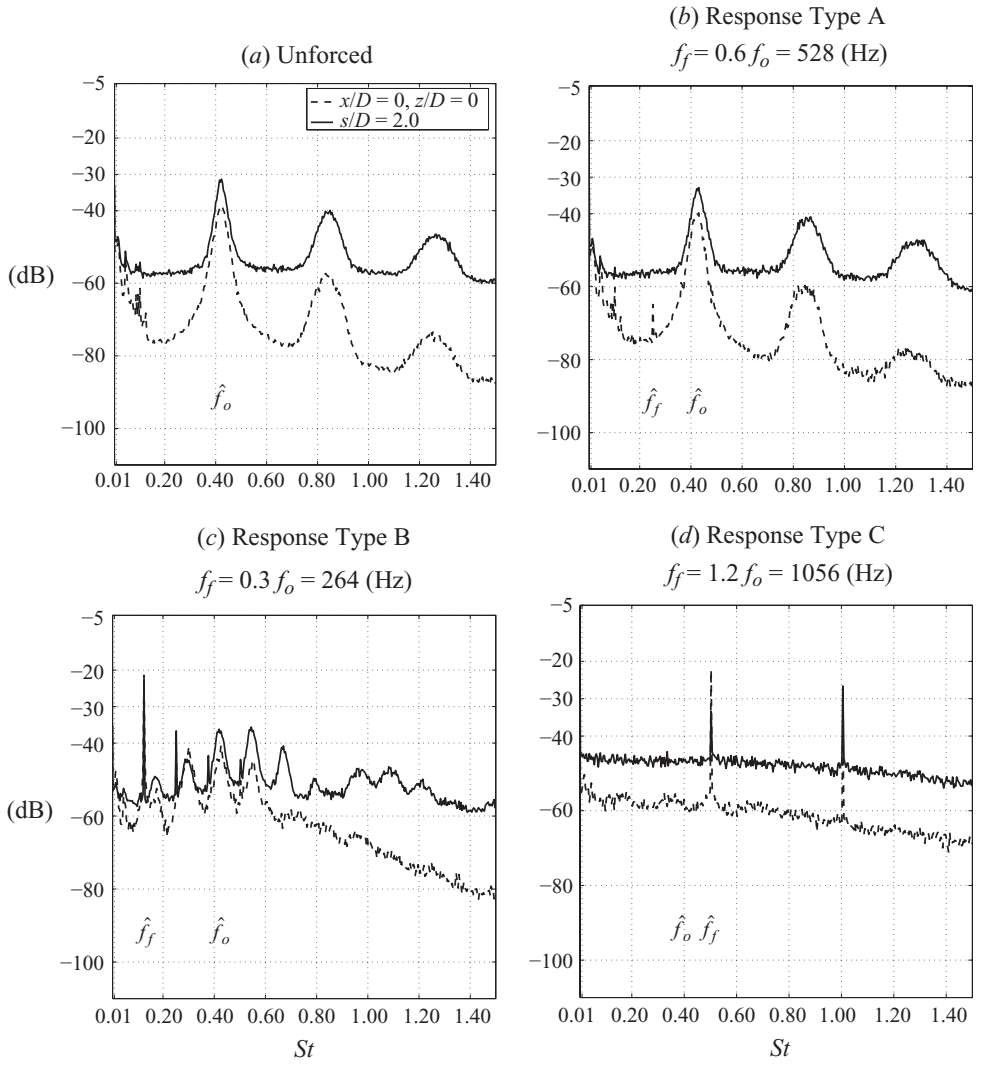

FIGURE 11. Upstream shear-layer spectra at $R = 1.15$ for: (*a*) no external forcing. (*b*) Excitation at frequency $f_f = 0.6 f_o$ and forcing amplitude equivalent to 1 % of the mean jet velocity, an example where the peak at f_o was dominant. (*c*) Excitation at $f_f = 0.3 f_o$ and amplitude equivalent to 20 % of the mean jet velocity, an example where the peak at f_o was present but not dominant. (*d*) Excitation at $f_f = 1.2 f_o$ and amplitude equivalent to 20 % of the mean jet velocity, an example where the peak at f_o was invisible and that at f_f was dominant. Results in (*b*), (*c*) and (*d*) are typical of response types shown on the control map in figure 12(*a*).

much greater, increasing beyond that associated with the fundamental mode, although the fundamental was still clearly observed. In most cases for this type of response, the r.m.s. of the perturbation velocity downstream along the shear layer, e.g. at $s/D = 2.0$, was greater than that for the unforced transverse jet at the same location, but occasionally the reverse was observed. Finally, when the jet was forced at very high amplitudes and/or at frequencies closer to f_o, it was possible for the forcing frequency (and its harmonics) to completely take over the spectral character of the shear layer, e.g. as shown in figure 11(*d*), with no visible evidence of the unforced

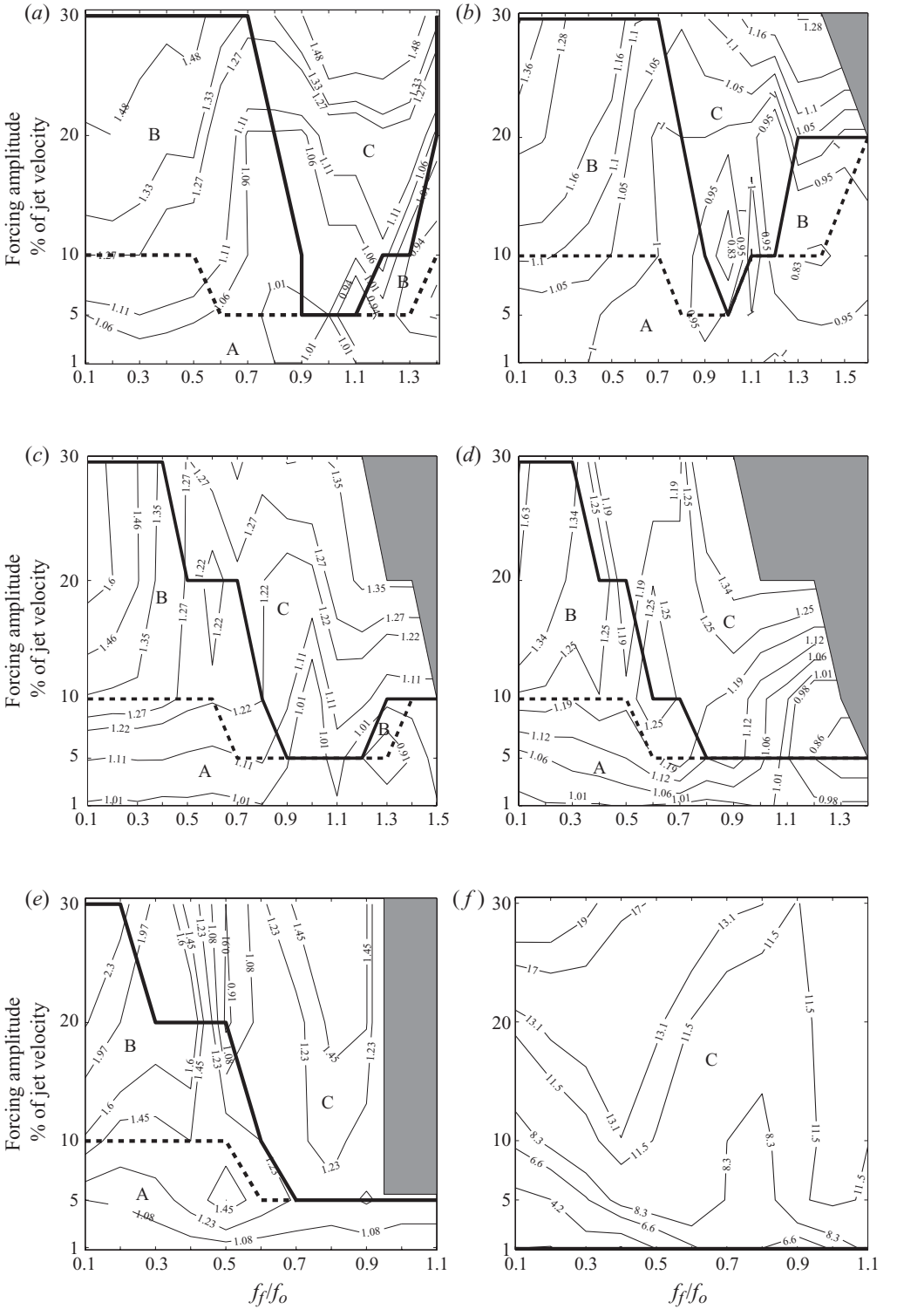

FIGURE 12. For caption see next page.

disturbance at frequency f_o. This represents conditions in which the global mode of the transverse jet 'locks in' to the forcing frequency f_f, as observed for low-density free-jet response examined by Juniper *et al.* (2009).

The alternate types of responses to forcing shown for $R = 1.15$ in figure 11(*b–d*) were observed for a wide range of values of f_f and forcing amplitudes for the transverse jet with $R \lesssim 3.0$; these three types of responses may be labelled as response types A, B and C, respectively. A summary of the forcing conditions under which shear-layer response corresponded to response types A, B and C for $R = 1.15$ is shown in the control map in figure 12(*a*). The contour lines with numbers correspond to conditions with a constant ratio of u'_{rms} with forcing to that without forcing, as measured at the upstream shear-layer location $s/D = 2.0$. In figure 12(*a*), the positions of the labels A, B (left side), and C on the contour map correspond approximately to the specific excitation conditions shown in figures 11(*b*)–11(*d*), respectively. Control maps for transverse jets with successively increasing R values are shown in figure 12(*b–f*). For globally unstable transverse jets ($R = 1.15$, 1.20, 1.50, 2.0 and 2.5 in figures 12(*a*)–12(*e*), respectively), response types A, B and C were clearly visible in the spectra, with the type C flow regime increasing in size with increasing R. The approximate boundaries of the type C response region are similar to those for the low-density jet (Hallberg & Strykowski 2008; Juniper *et al.* 2009). The near-linear relationship between forcing amplitude and frequency (or $|f_o - f_f|$) associated with lock-in is typical of a Hopf bifurcation to a global mode, as outlined in Huerre & Monkewitz (1990). As noted, there were a few conditions where $f_f \gtrsim f_o$ and where the local u'_{rms} with forcing was actually smaller than that without forcing at $s/D = 2.0$, despite the fact that the spectral amplitude at f_f was greater than that for the unforced jet at frequency f_o. This same kind of observation for certain forcing conditions is made by Hallberg & Strykowski (2008) for the low-density jet.

In the present experiments, when the transverse jet was in the convectively unstable regime, e.g. when $R = 6.4$, as in figure 12(*f*), the forcing frequency clearly overtook the natural mode under all forcing frequency and amplitude conditions, even those at very low excitation conditions. This behaviour confirmed for a wide range of frequencies the observations described in Megerian *et al.* (2007) for convectively unstable transverse jets. Yet when $R \lesssim 3.0$, responses to forcing as indicated in figure 12(*a–e*) were remarkably similar to that for other globally unstable flows.

4. Discussion and conclusions

The present experiments on the isodensity transverse jet provided ample new evidence for a clear transition in the flush jet's shear layer from being convectively unstable at jet-to-crossflow velocity ratios R exceeding about 3.3 to being absolutely

FIGURE 12. Control map for transverse jet response to sinusoidal forcing under different flow conditions. Contour lines correspond to the ratio of u'_{rms} during forcing to that without forcing measured at $s/D = 2.0$, plotted on axes representing excitation velocity at the centre of the jet exit, as a percentage of mean jet velocity, versus forcing frequency f_f scaled by the unforced natural frequency f_o. Conditions producing shear-layer response types A, B and C are indicated in the different regions, with definitions of the response types shown in figure 11. The heavy solid lines here refer to type C response, the heavy dashed lines refer to type B response, and the grey shaded area lies outside of the range of the present experiments. ($R = 1.15$ (*a*), 1.20 (*b*), 1.5 (*c*), 2.0 (*d*), 2.5 (*e*) and 6.4 (*f*).)

unstable for R values at or below the range of 3.0–3.3. Spectral alterations and sharply increasing r.m.s. disturbance amplitudes at fixed locations along the jet, evolving shear-layer spectra along and around the jet, spatial development of the fundamental and subharmonic disturbances, and response to strong sinusoidal forcing all have pointed to this transition, beyond the evidence provided in Megerian *et al.* (2007). Variations in natural disturbance amplitude with reductions in R as well as alterations in required forcing amplitude depending on forcing frequency are consistent with a Hopf bifurcation to a globally unstable flow condition. While only data for the flush jet at Reynolds number 2000 were provided here, separate observations on the transverse jet's stability at higher Reynolds numbers and/or for the elevated jet (Megerian *et al.* 2007; Davitian 2008) suggest a similar type of transition for these other types of transverse-jet flows.

As with the low-density jet, the implications of this shear-layer transition for the ability to control transverse-jet behaviour are considerable. While it is clear from results such as those in figure 12(*a–f*) that strong sinusoidal forcing can be used to overcome the natural (unforced) global instabilities, the question of the impact of this strong forcing on the jet's visible features, including penetration and spread, remains. Prior studies (M'Closkey *et al.* 2002) on strong sinusoidal transverse-jet forcing at a single jet condition ($R \approx 2.58$) suggest that this type of forcing has little effect on jet behaviour, in contrast to square-wave forcing with the same r.m.s. amplitude of excitation. The present results suggest that strong sinusoidal forcing of a globally unstable transverse jet may simply replace one dominant mode for another (cf. figures 11*a* and 11*d*) with little overall impact. Exploration of the visible and quantitative effects of strong sinusoidal forcing of this globally unstable flow, in contrast to use of other temporal waveforms, is the subject of a separate study (Davitian *et al.* 2010).

The authors wish to acknowledge helpful discussions with and contributions of Professor Leonardo Alves of the Instituto Militar de Engenharia, Rio de Janeiro, Brasil and of Professor Robert Kelly of UCLA. Support for this project from the National Science Foundation under grants CTS-0457413 and CBET-0755104, and from the NASA Graduate Student Research Program, is gratefully acknowledged.

REFERENCES

Alves, L. S. 2006 Transverse jet shear layer instabilities: linear stability analysis and numerical simulations. PhD thesis, University of California, Department of Mechanical and Aerospace Engineering, Los Angeles, CA.

Alves, L. S. de B., Kelly, R. E. & Karagozian, A. R. 2007 Local stability analysis of an inviscid transverse jet. *J. Fluid Mech.* **581**, 401–418.

Alves, L. S. de B., Kelly, R. E. & Karagozian, A. R. 2008 Transverse-jet shear-layer instabilities. Part 2. Linear analysis for large jet-to-crossflow velocity ratio. *J. Fluid Mech.* **602**, 383–401.

Bagheri, S., Schlatter, P., Schmid, P. J. & Henningson, D. S. 2009 Global stability of a jet in crossflow. *J. Fluid Mech.* **624**, 33–44.

Broadwell, J. E. & Breidenthal, R. E. 1984 Structure and mixing of a transverse jet in incompressible flow. *J. Fluid Mech.* **148**, 405–412.

Camussi, R., Guj, G. & Stella, A. 2002 Experimental study of a jet in a crossflow at very low Reynolds number. *J. Fluid Mech.* **454**, 113–144.

Chomaz, J.-M. 2005 Global instabilities in spatially developing flows: non-normality and nonlinearity. *Annu. Rev. Fluid Mech.* **37**, 357–392.

Cortelezzi, L. & Karagozian, A. R. 2001 On the formation of the counter-rotating vortex pair in transverse jets. *J. Fluid Mech.* **446**, 347–373.

Davitian, J. 2008 Exploration and controlled excitation of transverse jet shear layer instabilities. PhD thesis, University of California, Department of Mechanical and Aerospace Engineering, Los Angeles, CA.

Davitian, J., Hendrickson, C., Getsinger, D., M'Closkey, R. T. & Karagozian, A. R. 2010 Strategic control of transverse jet flows. *AIAA J.* (to appear).

Fric, T. F. & Roshko, A. 1994 Vortical structure in the wake of a transverse jet. *J. Fluid Mech.* **279**, 1–47.

Hallberg, M. P. & Strykowski, P. J. 2008 Open-loop control of fully nonlinear self-excited oscillations. *Phys. Fluids* **20**, 041703.

Hammond, D. & Redekopp, L. 1997 Global dynamics of symmetric and asymmetric wakes. *J. Fluid Mech.* **331**, 231–260.

Ho, C. M. & Huerre, P. 1984 Perturbed free shear layers. *Annu. Rev. Fluid Mech.* **16**, 365–424.

Huerre, P. & Monkewitz, P. A. 1990 Local and global instabilities in spatially developing flows. *Annu. Rev. Fluid Mech.* **22**, 473–537.

Juniper, M. P., Li, L. K. B. & Nichols, J. W. 2009 Forcing of self-excited round jet diffusion flames. *Proc. Combust. Inst.* **32**, 1191–1198.

Kamotani, Y. & Greber, I. 1972 Experiments on a turbulent jet in a cross flow. *AIAA J.* **10**, 1425–1429.

Karagozian, A. R. 1986 An analytical model for the vorticity associated with a transverse jet. *AIAA J.* **24**, 429–436.

Kelly, R. E. & Alves, L. S. de B. 2008 A uniformly valid asymptotic solution for a transverse jet and its linear stability analysis. *Phil. Trans. R. Soc. Lond.* A **366**, 2729–2744.

Kelso, R. M., Lim, T. T. & Perry, A. E. 1996 An experimental study of round jets in cross-flow. *J. Fluid Mech.* **306**, 111–144.

Kelso, R. & Smits, A. 1995 Horseshoe vortex systems resulting from the interaction between a laminar boundary layer and a transverse jet. *Phys. Fluids* **7**, 153–158.

Kuzo, D. M. 1995 An experimental study of the turbulent transverse jet. PhD thesis, California Institute of Technology, Pasadena, CA.

Kyle, D. M. & Sreenivasan, K. R. 1993 The instability and breakdown of a round variable-density jet. *J. Fluid Mech.* **249**, 619–664.

Margason, R. J. 1993 Fifty years of jet in cross flow research. *AGARD-CP-534* **1**, 1–141.

M'Closkey, R. T., King, J., Cortelezzi, L. & Karagozian, A. R. 2002 The actively controlled jet in crossflow. *J. Fluid Mech.* **452**, 325–335.

Megerian, S., Davitian, J., Alves, L. S. de B. & Karagozian, A. R. 2007 Transverse jet shear-layer instabilities. Part 1. Experimental studies. *J. Fluid Mech.* **593**, 93–129.

Monkewitz, P. A., Bechert, D. W., Barsikow, B. & Lehmann, B. 1990 Self-excited oscillations and mixing in a heated round jet. *J. Fluid Mech.* **213**, 611–639.

Moussa, Z. M., Trischka, J. W. & Eskinazi, S. 1977 The nearfield in the mixing of a round jet with a cross-stream. *J. Fluid Mech.* **80**, 49–80.

Muppidi, S. & Mahesh, K. 2007 Direct numerical simulation of round turbulent jets in crossflow. *J. Fluid Mech.* **574**, 59–84.

Pier, B. 2003 Open-loop control of absolutely unstable domains. *Proc. R. Soc. Lond.* A **459** (2033), 1105–1115.

Provansal, M., Mathis, C. & Boyer, L. 1987 Benard-von Karman instability: transient and forced regimes. *J. Fluid Mech.* **182**, 1–22.

Shapiro, S., King, J., M'Closkey, R. T. & Karagozian, A. R. 2006 Optimization of controlled jets in crossflow. *AIAA J.* **44**, 1292–1298.

Smith, S. H. & Mungal, M. G. 1998 Mixing, structure and scaling of the jet in crossflow. *J. Fluid Mech.* **357**, 83–122.

Sreenivasan, K. R., Raghu, S. & Kyle, D. 1989 Absolute instability in variable density round jets. *Exp. Fluids* **7** (5), 309–317.

Strykowski, P. J. & Niccum, D. L. 1991 The stability of countercurrent mixing layers in circular jets. *J. Fluid Mech.* **227**, 309–343.

Strykowski, P. J. & Niccum, D. L. 1992 The influence of velocity and density ratio on the dynamics of spatially developing mixing layers. *Phys. Fluids* A **4** (4), 770–781.

Yuan, L. L. & Street, R. L. 1998 Trajectory and entrainment of a round jet in crossflow. *Phys. Fluids* **10**, 2323–2335.

Ziefle, J. & Kleiser, L. 2009 Large-eddy simulation of a round jet in crossflow. *AIAA J.* **47** (5), 1158–1172.